Magnetotaxis for Nanofabrication

Isaac G. Macwan, Zihe Zhao, Omar T. Sobh and Prabir K. Patra

Abstract— **Magnetotactic bacteria (MTB), discovered in early 1970s contain single-domain crystals of magnetite (Fe_3O_4) or greigite (Fe_3S_4) called magnetosomes ranging from 35 to 120 nm in size. These crystals tend to form a chain like structure from the proximal to the distal pole along the long axis of the cell and align through an acidic protein mamJ to the bacterial cytoskeleton filament made out of actin-like protein mamK. The ability of these bacteria to sense the magnetic field, also called magnetotaxis, arises from the magnetic dipole moment of the entire chain of magnetosomes acting as a large magnet. Such organisms being facultatively anaerobic are able to sense the geomagnetic field and traverse the oxic-anoxic interface in aquatic habitats for optimal oxygen concentrations. Two aspects that are of particular interest are their phenomenal control of direction using magnetic field as well as the efficient displacement of selective nanoparticles. We aim to understand the efficacies of *Magnetospirillum magneticum* (AMB-1) in miniaturized semiconductor fabrication utilizing single and multi-walled carbon nanotubes.**

Index Terms—**Carbon nanotubes, Magnetospirillum, Magnetotaxis, Semiconductors**

I. Introduction

According to the semiconductor industry roadmap maintained by ITRS (International Technology Roadmap for Semiconductors), the feature size of a single transistor on a silicon wafer has reached 22nm in the year 2012. The NAND flash drives, MPU (Micro-Processor Unit) and DRAM (Dynamic Random Access Memory), which are the test vehicles for the succeeding technologies utilize a double-patterning (DP) technique to extend the wavelength of the exposure (which is otherwise 40-nm) and to keep a constant numerical aperture (NA) [1]. As the technology is scaled down below 22nm, it is during this time that unconventional non-lithographic or non-optical techniques become important because of the limitations such as the scattering of the EUV (Extreme Ultra-violet) light resulting in precision issues, need of a stringent vacuum environment to avoid contamination and the construction and capital equipment cost that increases by the orders of magnitude [2]. Newer technologies are already being explored to replace the silicon channel and source/drain regions with new, high mobility and high carrier velocity materials to sustain CMOS performance gains. Current chip manufacturing strategies can be divided into four major categories: (1) Conventional methods, where efforts are made to improve the current equipments to get better precision and resolution along with scaling of the MOSFETs such as double-patterning [3],[4],[5],[6], high-k dielectrics [7],[8], strained silicon [9],[10],[11],[12] and defects engineering [13], (2) New materials, where replacement materials such as carbon-based materials - graphene, carbon nanotubes, fullerenes and hydrogen saturated pentacene as well as hexabenzocoronene are used in place of conventional silicon-based materials [14]. Other materials such as microbial nanowire networks [15], organic single-crystals [16], DNA [17] and a combination of grapehene oxide, graphene, molybdenum disulphide (MoS_2) [18], Strontium Titanate ($SrTiO_3$) and silicon [19] are also being investigated for replacing the current silicon-only based materials, (3) Alternative methods, where new ways are explored for chip fabrication keeping the conventional working principles such as soft lithography [20], maskless lithography [21], molecular manipulation techniques [22], use of nanowires [23],[24] and tri-gate transistor technology [25], and (4) Self-assembly, which can be further categorized into absolute (total) self-assembly [26],[27] and directed self-assembly [28],[29].

Here we came up with an alternative approach where magnetotaxis (sensitivity to the magnetic field) of a bacterial species discovered in 1970s [30] is utilized for controlled navigation along a mesh of millimeter-sized solenoid coils made out of micrometer-sized thick conductors and in turn for selective deposition on a substrate. According to reference [31], the flagella bundles (FB) (about 12 – 20 nm in diameter) of MTB (magnetotactic bacteria) are able to produce a torque of approximately 4pN thereby displacing the cell giving it speeds ranging from 30 to 200μm/s depending on type of species and the number of magnetosomes. Our preliminary results indicate that AMB-1 (*Magnetosprillum magneticum*) may be utilized for precise control and navigation of the selected nano-particles such as single-walled (SW) and multi-walled (MW) carbon nanotubes (CNT) to achieve directed selective deposition. It is a non-lithographic technique that consists of two major interfaces, one between the bacterial entity and the CNT to be deposited and another between the CNT and the substrate (wafer). The former interface will guide the building material to the selected site over the substrate and the latter interface will aid the selective deposition. The purpose is to efficiently utilize the speed and

Manuscript received February 15, 2014.

I. G. Macwan is with the Department of Computer Science & Engineering, University of Bridgeport, Bridgeport, CT 06604 USA (Phone: 203-385-2129; e-mail: imacwan@my.bridgeport.edu).

Z. Zhao is with the Department of Computer Science, University of Bridgeport, Bridgeport, CT 06604 USA (e-mail: zihezhao@my.bridgeport.edu).

O. T. Sobh is with the Department of Biology, University of Pennsylvania, Philadelphia, PA 19104 USA (osobh@sas.upenn.edu).

P. K. Patra is with the Department of Mechanical Engineering and Biomedical Engineering, University of Bridgeport, Bridgeport, CT 06604 USA, (e-mail: ppatra@bridgeport.edu).

978-1-4799-5233-5/14/$31.00 ©2014 IEEE

size of these microorganisms to displace the molecules of semiconductor or compound semiconductor materials so as to selectively fabricate semiconductor components on a substrate. Our preliminary results indicate that such a compound technology involving bacterial carriers and organic/inorganic semiconductor molecules to fabricate information technology processing and memory units would be a possible alternative to the current EUV-based chip fabrication technology.

II. Micro-Organisms in Directed Manufacturing

In the past, efforts have been made to attach a bacterial species to plastic substrates such as polystyrene to study the cell hydrophobicity [32]. It demonstrated that one of the forces that is very common at the molecular level is the hydrophobic interactive force between the atoms. A form of algae (*Clamydomonas Reinhardtii*) has also been used as a carrier for polystyrene micro-beads (1-6μm diameter) that were carried to as far as 20 cm [33]. The micro-beads were attached to the algae cell using surface chemistry linking fragments of methyl ketone and a primary amide. Similarly, certain genetically engineered viruses have also been utilized for controlled ordering of the ZnS (Zinc Sulphide) nanocrystals at nanoscale up to micro and even centimeter scales [34]. In reference [35], attachment of polystyrene microbeads for simulating the speed and direction of the attached bacteria is explored. However, one particular class of bacteria called magnetotactic bacteria has been utilized relatively more than any other class mainly because of their effective control by magnetic fields. One of the first reports of the such species was back in 1994, where it was utilized in metal uptake showing that these bacteria can also act as orientation separators detecting upto 1ppm level of metal concentrations in the environment [36]. Like any other micro-organisms, MTBs have also been utilized for collective tasks. For e.g. in order to control the direction of flagellated MTBs (sp. MC-1, *Marine coccus*), a computerized controller is used that sends swarms of MTBs, which utilize the magnetic field generated by the current produced by the photovoltaic cells mounted on a micro-robot [37]. In this case, two V-shaped structures were moved close enough to each other by the MTBs thereby forming the letter 'M' in an aqueous solution. MC-1 have also been utilized in realizing a biosensor for pathogenic bacteria, where individual cells are first attached to a polystyrene micro-bead, which is further used to pick the pathogenic bacteria from a solution [38]. Both MC-1 and MSR-1 (sp. *Magnetospirillum gryphiswaldense*) have been thoroughly tested for their attachment to polystyrene microbeads ranging from 2μm to 5μm from the viewpoint of their speeds and thrust forces [39]. Once the bacterium is attached onto the micro-component, the micro-component can be displaced over a surface and this is the strategy that is focused on in the present research work in order to direct the assembly of a semiconductor component.

Some of the other applications that MTBs have shown to direct the assembly of are stacking of micro-cubes to form a structure similar to ancient pyramids [40] and displacement of $100x20x15\mu m^3$ sized resin based micro-components [41].

III. Control of Magnetic Field and Influence of Heat on MTB Communities

It is well known that a current carrying conductor produces a concentric magnetic field if the conductor happens to be a straight wire as shown in Fig 1. According to Ampere's law, the line integral of the magnetic field, B with respect to change in length $d\boldsymbol{l}$ over a closed path is μ_0 times the current enclosed by the path:

$$\oint B \bullet dl = \mu_0 I_{enclosed} \tag{1}$$

The usefulness of (1) is in determining the current enclosed within a path without complicated integration, whereby magnetic field around a long straight conductor can be determined with respect to the radial distance R from the surface of the conductor by (2):

$$B = (\mu_0 I)/(2\pi R) \tag{2}$$

One of the major components of this research is the effective directional control of the magnetic field so as to anticipate the controlled movement of the bacterial species through the locally generated magnetic field. As can be seen from Fig. 1, a long straight conductor produces a magnetic field in concentric circles around the conductor and hence the required displacement of the species cannot be controlled efficiently, as the bacterial carriers would either move towards or away from the conductor. However, instead of a long straight conductor, if a coiled conductor is used, then the magnetic field can be linear as well as directional as seen from Fig. 2, which can aid in the displacement of the carriers. It is known that the magnetic field through a coiled conductor having N turns can be modeled as in (3):

$$\oint \vec{B} \cdot \vec{dl} = \mu_0 \, \mathrm{N} \, \mathrm{I} \tag{3}$$

From Fig. 2, it can be seen that the magnetic field through a coiled conductor is concentrated mainly along the axis of the coil and also in an opposite direction along the periphery of the coil, in both cases acting linearly, thereby giving a better efficiency for the directional movement of the bacterial species.

The effect of heat on the community of magnetotactic bacteria is equally important and can be considered as a second important component for the present research after the directional control of the magnetic field because the bacterial species should be able to displace efficiently under the influence of the heat generated by the current carrying solenoid coils. Short term effects of temperature on the abundance and diversity of MC-1 revealed the presence of four altogether different operational taxonomic units in one study [42]. Based on the results from four different temperature microcosms having identical conditions, it was found that 9 □ C, 15 □ C and 26 □ C temperature had relatively no effect on the MC-1 community. However, at 37

□ C, the number of MC-1 cells reduced drastically with several other taxonomic units coming into play.

The temperature rise due to the current flowing through a conductor can be determined from the first principles using the mass (volume (Area x Length) and material density) of the conductor and the heat liberated, *W* in the conductor can be determined using the action integral of the current and the resistivity, *R* of the conductor. Finally, the temperature rise, *T* can be determined by using the mass of the conductor and the specific heat as a result of injecting certain amount of heat, *W*:

$$T = \text{joules} \times 0.2389 \times W \quad (4)$$

It is known that the temperature co-efficient of resistivity is to be taken into account while calculating the final value of the temperature rise. The value obtained from (4) is to be reused to determine the changed value of the resistivity and based on this new value of resistivity, a new temperature rise must be calculated. Normally this cycle is repeated till the melting point of the material is reached. However, based on the reference [42], the MC-1 had a drastic change in the abundance as well as the diversity at only 37 □ C. Hence, the number of iterations for calculating the final temperature rise due to the current flowing through the solenoid can be bounded at the upper limit in a relatively short time frame. It is already known that the cultivation of such bacteria requires a temperature up to 30 □ C. Thus, based on this information alone, the ability of the bacteria to survive beyond this temperature limit can be gauged. However, there is a relationship involved between the efficient motion of the species and the temperature rise that needs to be explored further in order to determine the cut-off limit for the rise in temperature. As a matter of fact, a study conducted with a light source on one side and the heat source on the other side of the MTB culture showed that the AMB-1 cells moved simultaneously towards both the light source indicating an efficient phototaxis and towards the heat source as well [43]. Furthermore, it was demonstrated that the phototaxis is independent of the magnetotaxis.

IV. Materials and Methods

A. AMB-1 Cultivation

AMB-1 (*Magnetospirillum magneticum*) (ATCC-700264) is a bipolar microaerophilic (facultatively anaerobic) micro-organism of the phylum α-proteobacteria. This particular bacteria was selected due to their unique ability to grow both aerobically and anaerobically and their superior control through magnetotaxis due to the presence of nanoscale magnetite (Fe_3O_4) within the bacterial cell. The cultivation protocol as given by ATCC (American Type Culture Collection) for the revised MSGM (Magnetospirillum Growth Medium) was utilized both for the liquid as well as semisolid media preparation. The culture protocol is as shown in TABLE I (per 1L of distilled water). After adding the chemicals, the media is checked for the pH, which should be 6.75 and if needed, 0.5M NaoH is used to set the pH using a pH-meter. The media is then autoclaved at 121□ C for 15 minutes and about 1ml of inoculum is injected to a 10ml screw-cap test tube aseptically. The test tube is filled to the top leaving less than 1ml of headspace and is tightly screwed to have a microaerophilic condition. Finally, the culture is incubated at a temperature 30 □ C. Resazurin is added to the media to keep track of the dissolved oxygen. Initially the media with resazurin has a blue tinge of color but after a while it turns to pink and stays that way to indicate the presence of dissolved oxygen. If the conditions inside the test tube are close to anaerobic, the blue tinge transforms to a colorless solution. Ferric quinnate is the primary iron source for AMB-1 that is sequestered by the siderophores released by the cells, which when binds with the iron particle are received at the receptors on the bacterial surface [44].

Semi-solid media culture method is used for checking the motility of cells and metabolic research. The solidity of semi-solid medium is between solid medium and liquid medium and as it is softer than solid media, semi-solid media allow bacteria to move freely and hence leave a trace of their displacement inside the media. Bacteria which are inside the semi-solid media will exhibit a cloudy haze or increase in turbidity, which show the location of the bacteria based on which motility can be determined. AMB-1 can be cultured in semi-solid medium using a screw-cap test tube for investigating the metabolic type, where 10ml of semi-solid medium is injected into the screw cap test tube and autoclaved at 121 □ C for 15 minutes after which it is left for cooling at room temperature. AMB-1 cells can be inoculated when the medium cools down to the room temperature through a clean transfer loop, where the medium is gently penetrated in the vertical direction making sure that the transfer loop does not touch the inner sides of test tube. After inoculation, the test tubes are incubated at 30 □ C for 2 days.

In a similar manner, culturing using a semi-solid medium in a petri dish is used for motility testing. Medium is autoclaved at 121□ C for 15 minutes and about 5mm deep semi-solid medium is added into the petri dish before it cools down, after which it is left at room temperature for cooling. One loop of bacteria is taken by transfer loop that rips the semi-solid medium in the middle of the Petri dish and then the petri dish is left in a candle jar beside a magnet under anaerobic conditions at incubation temperature of 30 □ C for 2 days.

B. Estimation of Cell Density and Cell Growth

The number of cells (cell density) can be checked from time to time using a UV/Vis (Ultraviolet/Visible) spectrophotometer device that gives optical density (OD) measure with distilled water as a control. It is known that as the cells multiply, the media is no longer transparent but a haze (cloudiness) is seen as part of the increased cellular density. Due to this haziness, the OD reading increases, which depends also on the wavelength of light used. Generally, 600nm OD measurements are performed for bacterial cell growth and to determine the cellular density. A 3ml cuvette is filled with distilled water and another similar cuvette is filled with the cell culture. Both the cuvettes are placed in the path of the focused light beam, which penetrates the solutions and determines the optical density. A graph of time versus the OD is prepared to measure the growth phase, stationary phase and post-stationary phase. After the stationary phase has elapsed,

the number of efficient cells start to decrease, which in turn sets a time constraint for the next sub-culturing cycle. A part of incident light's energy is absorbed by the bacteria when the incident light proportional to the optical density (OD) penetrates the liquid culture. OD_{600nm} is the value of optical density at the incident light wavelength equal to 600nm that is the maximum absorption wavelength or the absorption peak for most of the bacteria and is widely used on bacteria density detection procedures.

C. Determination of Cellular Shape and Characteristics

The initial screening of the AMB-1 cells is done using optical microscopy techniques, where a wire-loop full of cells is taken on a clean glass-slide and heat-fixed through a burner. After heat-fixation, a crystal violet dye is used to coat the outer cell membranes of the cells for 40 to 60 seconds and flashed with water. Once the sample is prepared, the slide is kept under the light microscope for study with 100X oil-immersed lens. The smear could be observed under the microscope after the slide has dried. AMB-1 cells have a distinct spiral shape and each cell is between 4 to 10μm in length.

Apart from the cellular shape, it is also possible to check whether the bacteria is gram-negative or positive depending upon which, certain characteristics can be anticipated. It is the most important differential stain used in bacteriology. One drop of AMB-1 inoculum is placed on a glass slide on which drying and fixing with a burner flame is performed. Crystal violet is used for primary stain and is kept for one minute after which the slide is washed with water. Next, gram's iodine is applied and the slide is washed again after 1 minute. Decolorization of the smear is done using 95% ethyl alcohol until the alcohol runs almost clear. After washing the slide gently with water, counterstain in the form of safranin is applied for 45 seconds. The slide is now washed, dried and is observed under oil immersion (100X).

D. Initial Verification of Magnetotaxis

Magnetotaxis can be verified for individual AMB-1 cells utilizing either a permanent magnet or electro-magnet placed on the light microscope stage producing a magnetic field slightly higher than the geomagnetic field of 0.5G (0.5 Gauss). AMB-1 cells not only exhibit magnetotaxis but also aerotaxis and phototaxis. Hence, in order to have magnetotaxis as a dominant feature, it is necessary to apply weak uniform magnetic field above geomagnetic field so that photo- or aero-taxis do not come into play which is usually the case at higher magnetic fields. Unlike, the staining procedures, in this case, the cell suspension is utilized in a hanging drop assay. A hanging drop assay is a laboratory technique to determine the motility of the cells, where a specialized glass slide having a concave cavity is used and a drop of cell suspension is placed on a cover-slip, over which the glass slide is placed and the entire assembly inverted so that the drop containing cells remains hanging between the cover-slip and the glass slide. The living bacterial cells inside the drop can be examined under the effect of magnetic field, where changing the polarity of the field exhibits a change in the motility direction of the cells.

Apart from a simple hanging drop assay to determine the cellular motility, two more techniques are developed called the capillary racetrack (Fig. 3) and cross-micro-slide (Fig. 4). Capillary racetrack method is an effective way to separate motile MTB cells from other cells. Capillary racetrack device has two connected parts which are racetrack and sample holder. Racetrack is a 5 cm long capillary that has 1 to 2 mm inner diameter. One side is sealed and another side is connected to a sample holder having a 1cm diameter, where fresh sterilized liquid culture medium is filled.

0.5ml AMB-1 sample is injected into the sample holder and the device is kept in a uniform magnetic field of ~4G for magnetic separation of motile AMB-1 cells for 15min. 1 cm of the capillary racetrack tip is cut off after 15min and a hanging drop slide is made with the sample inside the 1 cm capillary racetrack tip, which is checked under optical microscope for the presence of magnetosensitive AMB-1 cells. Fig. 3 shows the schematic of a capillary racetrack with a culture medium in the sample holder (Fig. 3A) and motile AMB-1 cells that traveled to the end of the tip under the influence of a uniform magnetic field (Fig. 3B).

Similarly, a cross micro-slide technique as shown in Fig 4 is the one where four glass-slides are kept in a crisscross configuration with a permanent magnet at the centre, the magnetic field intensity of which is measured by a gaussmeter and marked at the respective points over the glass slides. 0.1ml AMB-1 sample is added on each slide taking care that the sample drop has long and narrow shape which can provide long track and thick liquid layer. Long track could allow MTB longitudinal displacement but limit horizontal movement and the thick liquid layer could extend drying time, which gives MTB more time to move. After addition of the sample and keeping the cross slides configuration in the magnetic field at room temperature for 5min, the long track on each glass slide is cut into three pieces using sterilized cotton swab. The MTB would be isolated in the three pieces after drying. Crystal violet is used for sample staining and the cell density for the three sections is checked under optical oil immersion microscopy.

E. Characterization of individual AMB-1 Cells and Magnetosomes

Based on the cellular shape of AMB-1 cells from optical microscopy and their efficient sensitivity to the applied magnetic field, the next step would be to characterize individual cells using electron microscopy (SEM and TEM) and atomic force microscopy (AFM) along with elemental analysis of individual magnetite crystals inside the cells through XRD (X-Ray Diffraction) elemental analysis. Scanning Electron Microscope (SEM) can show the morphology of the surface of the bacterial cell. The sample preparation for the SEM has six steps in general, which are chemical fixation, wash, dehydration, mounting, coating and imaging. Glutaraldehyde is used for chemical fixation. About 800μl of AMB-1 inoculum is centrifuged at 3000rpm for 3min, discarding the supernatant and the pallet is washed about 2 or 3 times with a 500μl 1×PBS solution. Next 1ml of 4% glutaraldehyde is added into the sample and is uniformly mixed after which it is frozen at 4 □ C for at least 4h. This cycle of centrifugation - PBS wash - freeze is repeated one

more time but now with freezing procedure with 500µl of 2% glutaraldehyde for 1h. Next, the sediment is washed with 1×PBS 3 more times. In the next step, gradient dehydration is performed with four different concentrations of alcohol, each time the sample is held for 10min and centrifuged at 3000rpm for 3 min. Finally, the sample is dissolved in Tert-Butanol. After mounting the sample on the SEM stub, it is coated with gold nanoparticles for enhanced imaging when observed under SEM.

For the TEM, usually it is needed to section the sample using a microtome or similar device. However, for the AMB-1 cells intended for the present study, once the SEM sample preparation protocol is performed, the sample could be directly mounted on the TEM carbon coated grid. Once dried, it could be observed under the TEM for investigation into the structure of internal organelles of the AMB-1 cells. With a high magnification of about 50nm, individual magnetite crystals can be observed along with their shape, size and crystal faces.

AFM, unlike SEM or TEM gives an excellent insight into the living cell in a pseudo-native environment. It not only determines the topography of the bacterial cell surface but also measures the height profile of the cell, thereby giving an exact shape and size of the bacterial cell through both non-contact and tapping modes. Using AFM in magnetic mode allows the use of magnetic tip to perform magnetic analysis of the magnetosome dipole on the living cells. The contrast on the phase image of the MFM (Magnetic Force Microscopy) would give useful insights into the polarity of the individual magnetosome as well as bacterial cell as a whole. Furthermore, the use of Force-Distance measurement technique in MFM/AFM gives an excellent understanding about the different long range and short range forces from and to the bacterial cell including adhesion, magnetic and electrostatic. This data would give an understanding on the force profile of the bacteria in aqueous media and the binding forces between the cell and carbon nanotube, which could further be compared with the simulated results.

F. Simulation of Magnetic Field, Associated Temperature Rise and Binding Kinetics Between AMB-1 and CNT

Efficient control and intensity of the magnetic field is a key element in this research work as the AMB-1 cells are highly sensitive to the locally generated magnetic field. In order to create both effective and efficient magnetic field environment, permanent magnets or electromagnets can be used. However, using such magnetic sources does not allow efficient control over the intensity and directionality of the field. In order to achieve this, copper coils made up of 44 AWG (American Wire Gauge) conductors are used and are analyzed through Finite Element Analysis (FEA) using COMSOL. The results provide a detailed analysis of the directionality and intensity of the magnetic field based on which real-time experiments can be conducted. Furthermore, simple magnetic field calculations for the number of coil turns, current through the coil and length of the coil involve a four-dimensional matrix problem and hence such calculations are taken care of by MATLAB.

Second most important aspect of this research work is the phenomenon of heat generation mainly due to the current flowing through the coil. The associated temperature rise may cause a temporary inactivation of the magnetotaxis of the AMB-1 cells causing them to lose their intended path. Again, the problem of heat generation and associated temperature rise being a FEA problem is dealt with FEA simulations, where based on the current flow and the characteristics of the copper material as well as surrounding media, the resulting heat generation would put constraints on the maximum allowable current, density of the number of turns and hence the generation of effective magnetic field to drive the bacterial carriers.

V. Results and Discussion

A. AMB-1 Cultivation

After the AMB-1 bacteria was inoculated at 30 □ C for 5 days, we could easily find that the medium in test tube 1 (control) was still clear but test tube 2 was getting turbid (Fig. 5(A)). Application of magnetic field via a small permanent magnet for 3 minutes to test tube 2 did not change anything whereas when the test tube 3, which was also getting turbid, was placed in a similar magnetic field, a visible dark spot was found above the magnet as shown in Fig. 5(B). These results indicated that the environment of test tube 2 could allow AMB-1 cells to grow but they had lost their sensitivity to the magnetic field (magnetotaxis). However, test tube 3 could not only provide a favorable condition to grow for the AMB-1 bacteria but also could conserve their magnetotaxis. The major difference between test tube 2 and test tube 3 was that the oxygen concentration in test tube 2 was large as compared to test tube 3 because test 2 was only partially filled with the media (there was a head space of about 5ml) whereas test tube 3 was totally filled (no head space for air/oxygen) proving that AMB-1 cells are facultatively anaerobic bacteria and hence they need a very minute amount of oxygen for their proliferation provided by the dissolved oxygen in the totally filled test tube, which was just enough for the micro-organisms to sequester required quantities of iron from the surrounding environment (media) and biomineralize the magnetosomes. On the other hand, keeping a headspace in the test tube would provide enormous quantities of oxygen, which would halt their production of magnetosomes and hence are no longer sensitive when grown aerobically.

AMB-1 cells were also cultured in a semi-solid media using a test tube for the metabolic type investigation and using a petri dish for testing the motility. In case of a petri dish, after 3 days of microaerobic cultivation under the influence of magnetic field, cells were found only on one side of the dish as shown in Fig. 5(C) confirming that AMB-1 could conserve magnetotaxis in microaerobic conditions. AMB-1 were inoculated in a test tube containing the semi-solid media and were incubated at 30 □ C for 2 days after which the position of the bacteria was checked. AMB-1 cells showed turbidity right below the semi-solid medium surface as shown in Fig. 5(D) indicating that these are microaerophilic in nature.

B. Morphological Observations of AMB-1 Cells

AMB-1 cells are easy to be stained by crystal violet, in which case there is no other additional chemical required if a

quick examination of their cellular shape is to be done. As per the optical microscope observation, AMB-1 cells have spiral shape with a difference in the length of the individual cells according to the growth phase as shown in Fig. 6(A). In gram staining it shows up as a gram-negative strain as shown in Fig. 6(C) and the SEM analysis determined the size of AMB-1 cells to be between 4 to 6 μm as shown in Fig. 6(B). However, the longest of the cells are up to 10μm in length as displayed by the TEM analysis in Fig. 6(D). The internal organelles called magnetosomes are clearly visible. High resolution imaging of the individual magnetosome shows the crystal that is about 40nm in size as shown in Fig. 6(E).

C. *Motility Test*

Utilizing an optical microscope and the capillary racetrack method, AMB-1 strain consisting of motile cells, which are sensitive to magnetic field can be reliably separated. Also capillary racetrack method could filter the magnetic AMB-1 bacteria from other nonmagnetic bacteria in case of contamination. Inoculating only these separated highly magnetosensitive AMB-1 cells could also help to preserve purity along with high motility. The motion of AMB-1 cells thus separated was recorded through a hanging drop assay. The optical microscope was focused on the edge of the drop, where few cells were swimming randomly. When a permanent magnet was placed on the microscope stage beside the glass slide, AMB-1 cells gathered to the edge and they followed the magnet all the way to the other side as depicted in Fig. 7 (A), (B) and (C). Similarly, the results of the cross micro slide method are as shown in Fig. 7(D) showing the difference in cellular density among the three sections on the slide. Section 1 has the highest number of cells, and the cellular density decreases in sections 2 and 3. This implies that AMB-1 cells always move along the magnetic field lines and towards the nearest magnetic pole.

D. *Simulation of magnetic field and heat for copper coils*

It is a known fact that a magnetic field around a straight conductor will be concentric in nature. Thus, if a magneto-sensitive entity is to be moved along the magnetic field, it will simply circulate around a straight conductor making it difficult to control its direction. On the other hand if a coil is used, then the magnetic field lines will travel along the coil axis. Hence, a magneto-sensitive entity can now be directionally controlled in case of a current carrying coil. MATLAB is used to model the relationship between the magnetic field intensity, B, current through the coil, I and radial distance from the surface of the conductor, R showing the behavior of B as a function of R. The 3-D curve also shows the behavior of B with respect to I and R indicating that B will be increased as I increases and R reduces (Fig. 8A).

This complex relationship will govern not only the size and number of turns of the coil wire but also a limit to the radial distance beyond which MTBs will be difficult to control. Fig. 8(C) and 8(D) shows the magnetic field profile for a straight conductor and the relationship between current, length of the coil and number of turns for a copper coil in comparison to 8(A). Finite element analysis is done using COMSOL's AC/DC module. The resulting simulation results for copper coil in bacterial media are as shown in Fig 8(C) and 8(D).

VI. Conclusions

Based on the preliminary experiments and simulation results, it is anticipated that AMB-1 can be utilized for selective deposition tasks. Magnetotaxis of the individual AMB-1 cells can be controlled through a controlled magnetic field, where generation of localized magnetic fields through copper coils comes into play. MATLAB and COMSOL results for the generation of magnetic field and heat by the copper coils give useful insights into the directional control of the bacterial entities. Magnetic force microscopy as well as atomic force microscopy to detect precise turgor pressure that an individual cell exerts is underway, based on which a correlation between CNT loaded and unloaded AMB-1 cells would be resolved. Attachment and detachment of CNTs through simulated results of VMD/NAMD will provide a real-time insight into the binding energy and associated factors governing the attachment and detachment phenomenon at nanoscale. A hybrid alternative technology to the current lithographic strategy is envisioned where biological phenomena could be used to fabricate electronic circuits in the sub-10nm regime.

Acknowledgment

We would like to acknowledge Dr. Kim Kissliner from the Brookhaven National Laboratory for his valuable insights and guidance in transmission electron microscopy and Dr. Jinnque Rho from the department of Biology at the University of Bridgeport for helpful suggestions in AMB-1 cultivation.

References

[1] D. Chan, "ITRS Chapter: Lithography," in Future FAB International, 2012, pp. 81-84.

[2] Y. Wei and M. C. Kelling, "Overlay control beyond 20nm node and challenges to EUV lithography," in Future FAB International, 2011, pp. 41-47.

[3] M. Drapeau, V. Wiaux, E. Hendrickx, S. Verhaegen, and T. Machida, "Double patterning design split implmentation and validation for the32nm node.," presented at Design for Manufacturability through Design-Process Integration, 2007.

[4] M. Hori, T. Nagai, A. Nakamura, T. Abe, G. Wakamatsu, T. Kakizawa, Y. Anno, M. Sugiura, S. Kusumoto, Y. Yamaguchi, and T. Shimokawa, "Sub-40-nm half-pitch double patterning with resist freezing process," presented at Advances in Resist Materials and Processing Technology, 2008.

[5] W. Shiu, H. J. Liu, J. S. Wu, T.-L. Tseng, C. T. Liao, C. M. Liao, J. Liu, and T. Wang, "Advanced self-aligned double patterning development for sub-30-nm DRAM manufacturing," presented at Optical Microlithography, 2009.

[6] C. Fonseca, M. Somervell, S. Scheer, W. Printz, K. Nafus, S. Hatakeyama, Y. Kuwahara, T. Niwa, S. Bernard, and R. Gronheid, "Advances and challenges in dual-tone development process optimization," presented at Optical Microlithography, 2009.

[7] G. D. Wilk, R. M. Wallace, and J. M. Anthony, "High-k gate dielectrics: Current status and materials properties considerations," Journal of Applied Physics, vol. 89, pp. 5243-5275, 2001.

[8] M. V. Fischetti, D. A. Neumayer, and E. A. Cartier, "Effective electron mobility in Si inversion layers in metal-oxide-semiconductor systems with a high-k insulator: The role of remote phonon scattering," Journal of Applied Physics, vol. 90, pp. 4587-4608, 2001.

[9] S. E. Thompson, M. Armstrong, C. Auth, S. Cea, R. Chau, G. Glass, T. Hoffman, J. Klaus, Z. Ma, B. Mcintyre, A. Murthy, B. Obradovic, L. Shifren, S. Sivakumar, S. Tyagi, T. Ghani, K. Mistry, M. Bohr, and Y.

El-Mansy, "A logic nanotechnology featuring strained-silicon," presented at Electron Device Letters, 2004.

[10] R. Oberhuber, G. Zandler, and P. Vogl, "Subband structure and mobility of two-dimensional holes in strained Si/SiGe MOSFET's," Physical Review B, vol. 58, pp. 9941-9948, 1998.

[11] M. V. Fischetti, F. Gamiz, and W. Hansch, "On the enhanced mobility in strained-silicon inversion layers," Journal of Applied Physics, vol. 92, pp. 7320, 2002.

[12] M. L. Lee and E. A. Fitzgerald, "Hole mobility enhancements in nanometer-scale strained-silicon heterostructures grown on Ge-rich relaxed Si1-xGex," Journal of Applied Physics, vol. 94, pp. 2590-2596, 2003.

[13] V. Jindal, P. Kearney, A. John, and F. Goodwin, "Reducing defects in EUV mask blanks to enable high-volume manufacturing," in Future FAB International, 2012, pp. 46.

[14] M. Burghard, H. Klauk, and K. Kern, "Carbon-based field-effect transistors for nanoelectronics," Advanced Materials, vol. 21, pp. 2586-2600, 2009.

[15] N. S. Malvankar, M. Vargas, K. P. Nevin, A. E. Franks, C. Leang, B.-C. Kim, K. Inoue, T. Mester, S. F. Covalla, J. P. Johnson, V. M. Rotello, M. T. Tuominen, and D. R. Lovely, "Tunable metallic-like conductivity in microbial nanowire networks," Nature Nanotechnology, vol. 6, pp. 573-579, 2011.

[16] A. L. Briseno, S. C. B. Mannsfeld, M. M. Ling, S. Liu, R. J. Tseng, C. Reese, M. E. Roberts, Y. Yang, F. Wudl, and Z. Bao, "Patterning organic signle-crystal transistor arrays," Nature, vol. 444, pp. 913-917, 2006.

[17] X. Liu, R. Aizen, R. Freeman, O. Yehezkeli, and I. Willner, "Multiplexed aptasensors and amplified DNA sensors using functionalized graphene oxide: application for logic gate operations," ACS Nano, vol. 6, pp. 3553-3563, 2012.

[18] W. J. Yu, Z. Li, H. Zhou, Y. Chen, Y. Wang, Y. Huang, and X. Duan, "Vertically stakced multi-heterostructures of layered materials for logic transistors and complementary inverters," Nature Materials, vol. 12, pp. 246-252, 2013.

[19] B. M. Kim, T. Brintlinger, E. Cobas, M. S. Fuhrer, H. Zheng, Z. Yu, R. Droopad, J. Ramdani, and K. Eisenbeiser, "High-performance carbon nanotube transistors on SrTiO3/Si substrates," Applied Physics Letters, vol. 84, pp. 1946, 2004.

[20] Y. Xia and G. M. Whitesides, "Soft lithography," Annual Review of Materials Science, vol. 28, pp. 153-184, 1998.

[21] L. Pan, Y. Park, Y. Xiong, E. Ulin-Avila, Y. Wang, L. Zeng, S. Xiong, J. Rho, C. Sun, D. B. Bogy, and X. Zhang, "Maskless plasmonic lithography at 22nm resolution," Scientific Reports, vol. 1, 2011.

[22] S. I. Stupp and P. V. Braun, "Molecular manipulation of microstructures: Biomaterials, ceramics and semiconductors," Science, vol. 277, pp. 1242-1248, 1997.

[23] L. J. Lauhon, M. S. Gudiksen, D. Wang, and C. M. Lieber, "Epitaxial core-shell and core-multishell nanowire heterostructures," Nature, vol. 420, pp. 57-61, 2002.

[24] H. Yan, H. S. Choe, S. Nam, Y. Hu, S. Das, J. F. Klemic, J. C. Ellenborgen, and C. M. Lieber, "Programmable nanowire circuits for nanoprocessors," Nature, vol. 470, pp. 240-244, 2011.

[25] B. Doyle, B. Boyanov, S. Datta, M. Doczy, S. Hareland, B. Jin, J. Kavalieros, T. Linton, R. Rios, and R. Chau, "Tri-gate fully-depleted CMOS transistors: fabrication, design and layout," presented at Symposium on VLSI Technology, 2003.

[26] A. B. Parviz, R. Declan, and G. M. Whitesides, "Using self-assembly for the fabrication of nano-scale electronic and photonic devices," IEEE transactions on Advanced Packaging, vol. 26, pp. 233-241, 2003.

[27] L. Wei and A. M. Sastry, "Self-assembly for semiconductor industry," IEEE transactions on Semiconductor Manufacturing, vol. 20, pp. 421-431, 2007.

[28] P. A. Smith, C. D. Nordquist, T. N. Jackson, T. S. Mayer, B. R. Martin, J. Mbindyo, and T. E. Mallouk, "Electric-field assisted assembly and alignment of metallic nanowires," Applied Physics Letters, vol. 77, pp. 1399, 2000.

[29] H. Zhang, S. Boussaad, N. Ly, and N. J. Tao, "Magnetic-field assisted assembly of metal/polymer/metal junction sensors," Applied Physics Letters, vol. 84, pp. 133, 2004.

[30] R. Blakemore, "Magnetotactic Bacteria," Science, vol. 190, pp. 377-379, 1975.

[31] S. Martel, "Controlled bacterial micro-actuation," presented at International conference on Microtechnologies in Medicine and Biology, Okinawa, Japan, 2006.

[32] M. Rosenberg, "Bacterial adherence to polystyrene: a replica method of screening for bacterial hydrophobicity," Applied and Enivronmental Microbiology, vol. 42, pp. 375-377, 1981.

[33] D. B. Weibel, G. Piotr, R. Declan, D. R. Willow, M. Mayer, J. E. Seto, and G. M. Whitesides, "Microoxen: Microrganisms to move microscale loads," Proceedings of the National Academy of Sciences of the United States of America, vol. 102, pp. 11963-11967, 2005.

[34] S.-W. Lee, C. Mao, C. E. Flynn, and A. M. Belcher, "Ordering of quantum dots using genetically engineered viruses," Science, vol. 296, pp. 892-895, 2002.

[35] M. A. Traore and B. Behkam, "A stochastic model of chemotactic motion of micro-beads propelled by attached bacteria," presented at 3rd IEEE RAS and EMBS International conference on Biomedical Robotics and Biomechatronics (BioRob), Tokyo, 2010.

[36] A. S. Bahaj, P. A. B. James, and I. W. Croudace, "Metal uptake and separation using magnetotactic bacteria," IEEE transactions on Magnetics, vol. 30, pp. 4707-4709, 1994.

[37] S. Martel, W. Andre, M. Mohammadi, Z. Lu, and O. Felfoul, "Towards swarms of communication-enabled and intelligent sensotaxis-based bacterial microrobots capable of collective tasks in an aqueous medium," presented at IEEE International conference on Robotics and Automation (ICRA '09), Kobe, 2009.

[38] J. El Fouladi, Z. Lu, Y. Savaria, and S. Martel, "An integrated biosensor for the detection of bio-entities using magnetotactic bacteria and CMOS technology," presented at 29th Annual International Conference of the IEEE Engineering in Medicine and Biology Society (EMBS), Lyon, France, 2007.

[39] S. Martel, C. C. Tremblay, S. Ngakeng, and G. Langlois, "Controlled manipulation and actuation of micro-objects with magnetotactic bacteria," Applied Physics Letters, vol. 89, pp. 233904, 2006.

[40] S. Martel and M. Mohammadi, "Using a swarm of self-propelled natural microrobots in the form of flagellated bacteria to perform complex micro-assembly tasks," presented at IEEE International Conference on Robotics and Automation (ICRA), Anchorage, AK, 2010.

[41] E. K. Marvi, N. Mokrani, M. Mohammadi, and S. Martel, "Impact of the geometrical features of mciro-components in bacterial micro-assemblies," presented at 5th International Conference on MicroManufacturing (ICOMM/4M), Madison, Wisconsin, 2010.

[42] L. Wei, W. Yinzhao, and P. Yongxin, "Short-term effects of temperature on the abundance and diversity of magnetotactic cocci," MicrobiologyOpen, vol. 1, pp. 53, 2012.

[43] C. Chen, Q. Ma, W. Jiang, and T. Song, "Phototaxis in the magnetotactic bacterium magnetospirillum magneticum strain AMB-1 is independent of magnetic fields," Applied Microbiology and Biotechnology, vol. 90, pp. 269-275, 2011.

[44] R. J. Calugay, H. Miyashita, Y. Okamura, and T. Matsunaga, "Siderophore production by the magnetic bacterium magnetospirillum magneticum AMB-1," FEMS Microbiology Letters, vol. 218, pp. 371-375, 2003.

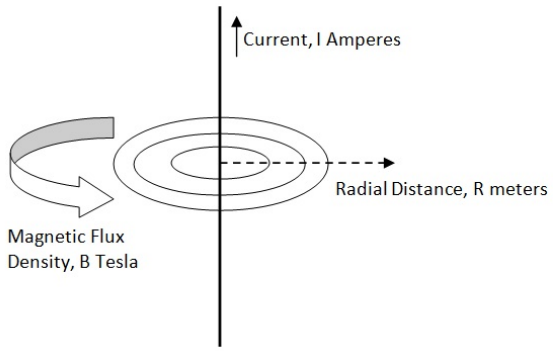

Fig. 1. Magnetic field around a long straight conductor

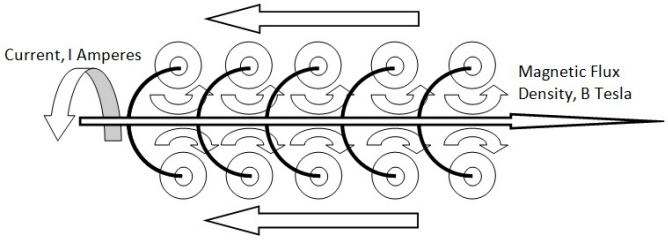

Fig. 2. Magnetic field through a coiled conductor

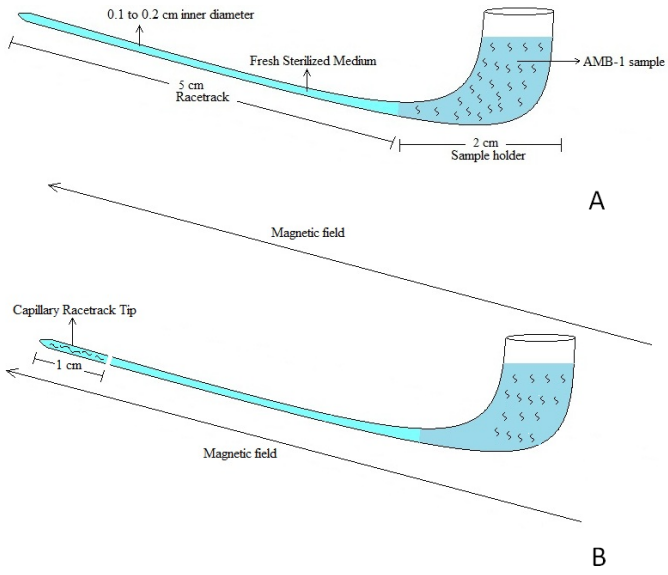

Fig. 3. Capillary racetrack technique: A- Sample holder with AMB-1 cells attached to the capillary racetrack; B- Capillary racetrack under the influence of uniform magnetic field. Magnetosensitive AMB-1 cells travel till the end of the tip, which is broken and the cells are studied under optical microscope.

TABLE I
MSGM (MAGNETOSPIRILLUM GROWTH MEDIUM) CULTIVATION PROTOCOL

Chemical	Quantity[a]
Wolfe's Vitamin	10ml
Wolfe's Mineral	5ml
0.01M Ferric Quinate	2ml
0.1% Resazurin	0.45ml
KH_2PO_4	0.68g
$NaNO_3$	0.12g
Ascorbic Acid	0.035g
Tartaric Acid	0.37g
Succinic Acid	0.37g
Sodium Acetate	0.05g
Agar (for semi-solid media)	1.3g

[a]Per 1000 ml of water

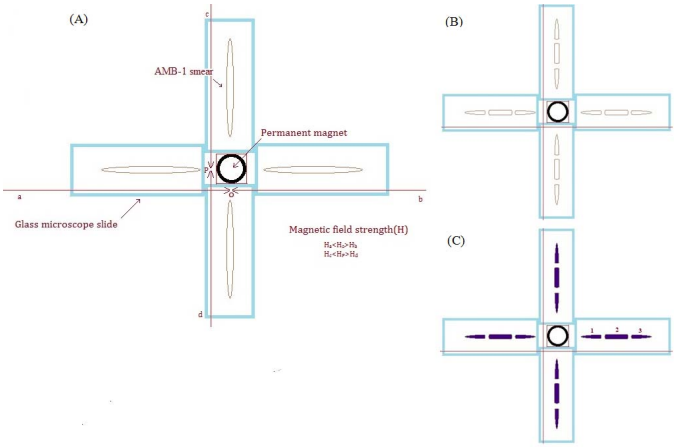

Fig. 4. (A) Crisscross glass slide arrangement showing four glass slides with a permanent magnet in the centre. The arrows indicate the direction of the field lines; (B) After slicing three sections per slide in order to get the cellular density in each of the sections; (C) Same configuration as in (B) after the application of crystal violet for observation under optical microscope.

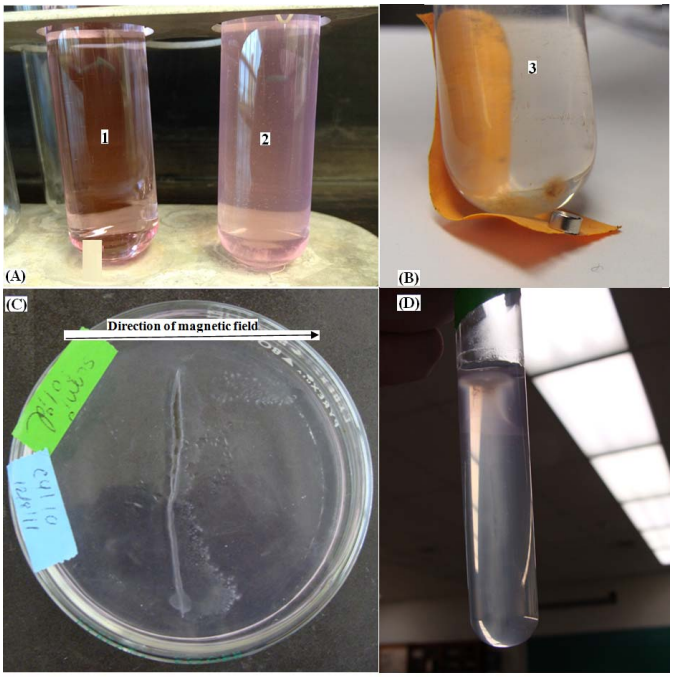

Fig.5. (A) Test tube 1 (control) showing clear media indicating no contamination whereas test tube 2 shows turbidity indicating that the AMB-1 cells have grown. (B) Test tube 3 shows a visible dark spot right over a permanent magnet indicating the magnetotaxis response of the AMB-1 cells. (C) AMB-1 cells cultured in a petri dish showing a visible vertical smear at the centre of the dish and cells migrating exclusively to the right side of the dish towards a magnetic pole confirming the magnetotaxis of the cells. (D) AMB-1 cells in a semi-solid media in a test tube showing visible tubidity right below the surface of the media confirming the microaerophilic nature of AMB-1 cells.

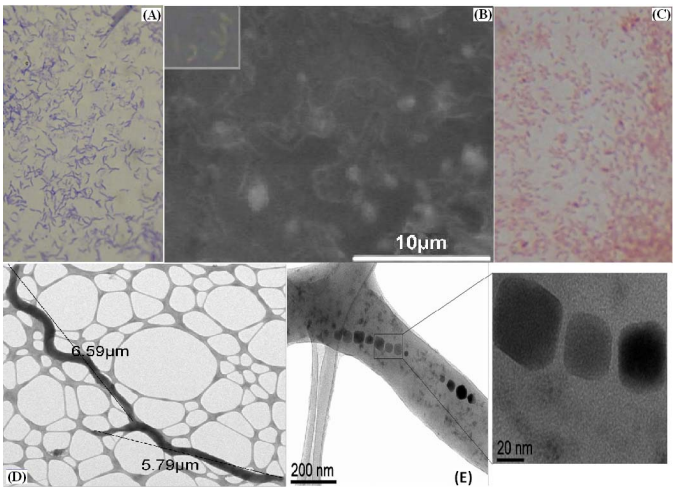

Fig. 6. (A) Simple staining of AMB-1 showing spiral morphology of the cells. Variations in the lengths are due to the different growth phases that the cells are going through. (B) SEM analysis of the AMB-1 cells clearly showing the spiral morphology. A comparison of the cell shapes with simple staining is done as indicated in the inset image. (C) Gram staining of the AMB-1 cells indicating gram-negative nature of the cells (red-colored) due to the application of counterstain called safranin. (D) Length of a mature AMB-1 cell. (E) TEM analysis of AMB-1 showing the intracellular magnetite (Fe_3O_4) crystals. The blown up view shows the morphology of individual crystals.

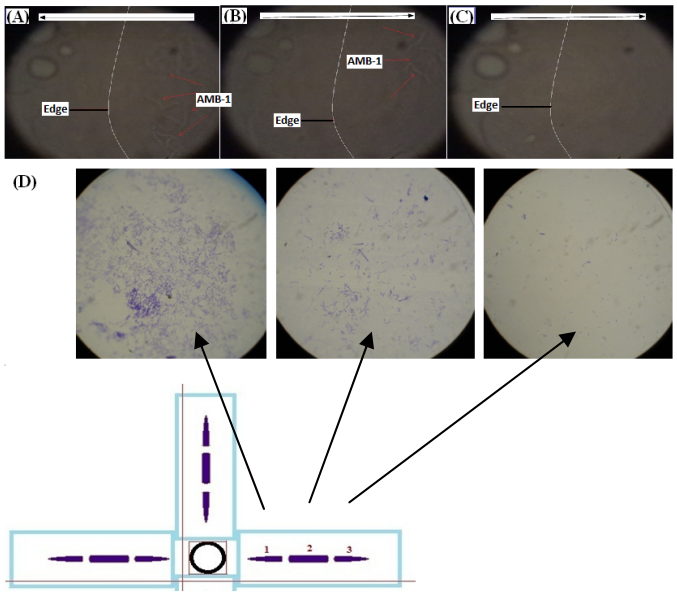

Fig. 7. (A) AMB-1 cells accumulated to the edge of the drop towards the magnet. (B) AMB-1 cells moving away from the edge, following the direction of the magnetic field. (C) No AMB-1 cells in sight indicating an efficient magnetotaxis. (D) Results of the CMS experiment indicating the increased cellular density near the magnet.

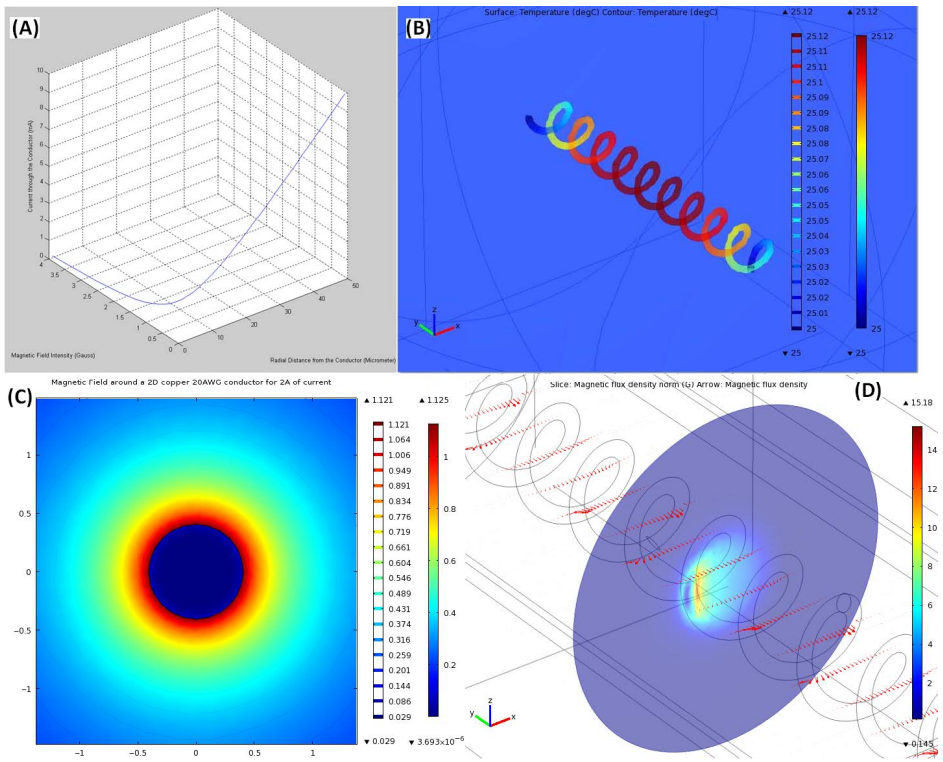

Fig. 8. (A) Magnetic field, B with respect to Current, I and Radial Distance, R using MATLAB, (B) Heat dissipated by a copper coil using COMSOL, (C) Magnetic field around a straight conductor in 2D, (D) Magnetic field around a copper coil.